International Journal of Modern Physics E

OPEN AND HIDDEN STRANGENESS PRODUCTION IN NUCLEON-NUCLEON COLLISIONS*

Radhey Shyam

Theory Division, Saha Institute of Nuclear Physics
1/AF Bidhan Nagar, Kolkata 700064, India
radhey.shyam@saha.ac.in

Received (received date)
Revised (revised date)

We present an overview of the description of K and η meson productions in nucleon-nucleon collisions within an effective Lagrangian model where meson production proceeds via excitation, propagation and subsequent decay of intermediate baryonic resonant states. The K meson contains a strange quark (s) or antiquark ($\bar{s}$) while the η meson has hidden strangeness as it contains some component of the $s\bar{s}$ pair. Strange meson production is expected to provide information on the manifestation of quantum chromodynamics in the non-perturbative regime of energies larger than that of the low energy pion physics. We discuss specific examples where proper understanding of the experimental data for these reactions is still lacking.

1. Introduction

It is well established that nucleons have a rich excitation spectrum which reflects their complicated multi-quark inner dynamics. The determination of properties of the nucleon resonances (e.g., their masses, widths, and coupling constants to various decay channels) is an important issue of the hadron physics. This will provide the benchmark for testing the predictions of the Lattice quantum chromodynamics (LQCD) which is the only theory which tries to calculate these properties from the first principles [1]. Even though, the requirement of the computational power is enormous for their numerical realization, such calculations have started to provide results for properties of ground as well as excited states of the nucleon [2,3]. Furthermore, reliable nucleon resonance data are also important for testing the "quantum chromodynamics (QCD) based" quark models of the nucleon (see, e.g. [4,5]) and also the dynamical coupled-channels models of baryonic resonances [6].

Experimental determination of baryonic resonance properties proceeds indirectly by exciting the nucleon with the help of a hadronic or electromagnetic probe

*Lecture presented in the 4th DAE-BRNS workshop on hadron physics, Aligarh Muslim University, Aligarh, India, Feb. 18-23, 2008

and performing measurements of their decay products (mesons and nucleons). The reliable extraction of nucleon resonance properties from such experiments is a major challenge. As description of the intermediate energy scattering is still far away from the scope of the LQCD calculations, the prevailing practice as of now, is to use effective methods to describe the dynamics of the meson production reactions. Such methods explicitly include baryon resonance states, whose properties are extracted by matching predictions of the theory with the experimental data. The ultimate goal is to compare the values extracted in this way with those predicted by the LQCD calculations.

In this lecture we review one such method which is based on an effective Lagrangian model [7], in the context of K and η meson (to be referred collectively as φ in the following) productions in elementary nucleon-nucleon (NN) collisions. In this model contributions to the amplitudes are taken into account by lowest order Feynman diagrams (tree-level) which are generated by effective Lagrangians that satisfy the relevant conservation laws and are consistent with the basic symmetry (chiral) of the fundamental theory, namely, the quantum chromodynamics (QCD). These Lagrangians involve baryons and mesons as effective degrees of freedom instead of quarks and gluons.

Recently, there has been a lot of interest in studying the production of φ mesons (which are the next lightest nonstrange members in the meson mass spectrum) in NN collisions and the corresponding data base has enhanced considerably (see, e.g., [8,9,10,11]). These reactions are expected to provide information on the manifestation of the QCD in the non-perturbative regime of energies larger than that of the pion physics where concepts like the low energy theorem and partial conservation of axial current (PCAC) provide a useful insight into the relevant physics [12]. The strangeness quantum number introduced by these reactions leads to new degrees of freedom into this domain which brings in new symmetries and conservation laws. They are expected to probe the admixture of $\bar{s}s$ pairs in the nucleon wave function [13,14] and the baryon-nucleon and φ-nucleon interactions [15].

The elementary $NB\varphi$ (B is a nucleon or hyperon) cross sections are one of the most crucial ingredients in the transport model studies of the φ-meson production in the nucleus-nucleus collisions [17,18,19,20]. They provide the opportunity to study the equation-of-state of the baryonic matter at high density [21] and in-medium modifications of strongly interacting particles which might be related to the chiral symmetry restoration [22]. These are the fundamental aspects of nuclear and hadron physics [23]. Furthermore, the enhancement of the open strangeness production has been proposed as a signature for the formation of quark-gluon plasma in high energy nucleus-nucleus collisions [24].

The elementary production reactions often provide important means for studying the properties of the nucleon resonances. For example, the spin-$\frac{1}{2}$, isospin-$\frac{1}{2}$, and odd parity nucleon resonance $N^*(1535)$ [$S_{11}(1535)$] has a remarkably large ηN branching ratio. It lies very close to the threshold of the $NN \to NN\eta$ reaction

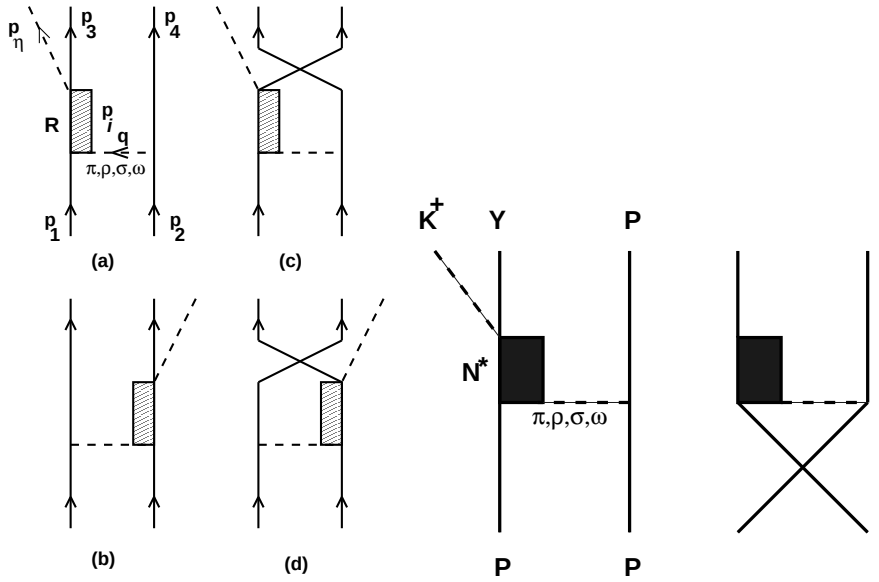

Fig. 1. Feynman diagrams for meson production in NN collisions. The graph on the left show 4 pieces of the η meson production; (a) and (b) are the direct target emission and projectile emission processes, while (c) and (d) are their the exchange counter parts. The graph on the right are the direct and exchange components of the kaon production.

and contributes to the amplitude of this reaction even at the threshold. Therefore, the study of η meson production in NN collisions at near threshold beam energies provides the unique opportunity to investigate the properties of $N^*(1535)$ which have been the subject of some debate recently (see, e.g., [16]).

The understanding of the elementary kaon production reactions is a doorway to the theoretical investigation of the production of hypernuclei in reactions like $A(p, K^+)_\Lambda B$ where the hypernucleus ${}_\Lambda B$ has the same neutron and proton numbers as the target nucleus A, with one hyperon added. Moreover, the attractive nature of the η-nucleon interaction may lead to the formation of bound (quasi-bound) η-nucleus states (see, e.g., [25,26,27,28,29]). This subject has been a topic of great interest recently. The formation of η mesic nuclei depend critically on the value of ηN scattering length ($a_{\eta N}$) (see, e.g., [30]). The η meson production in NN collisions near threshold energies provides vital information about $a_{\eta N}$.

2. Effective Lagrangian Model of Strange Meson Production in Elementary Collisions

The idea of the effective Lagrangian model is to account for the symmetries of the QCD by including only effective degrees of freedom instead of quarks. These effective degrees of freedom are modeled by baryons and mesons which exist as (quasi-)bound quark states. The advantage is that in this way one gets a better

insight in the underlying production mechanism which makes the interpretation of the results easier. However, due to more complicated interaction structure, the compliance of physical constraints like unitarity and analyticity becomes technically more involved. Enforcing unitarity dynamically requires solving a system of coupled equations with all possible final states. Recent coupled-channels approaches within an effective Lagrangian framework [30,31,32,33,34,35] are mostly confined to reactions leading to two-body final states. None of the effective Lagrangian models used to describe reactions leading to three-body final states involve in-built unitarity.

2.1. *Effective Lagrangians, Form Factors, Coupling Constants*

Within our effective Lagrangian approach, we consider the tree-level structure (Fig. 1) for the amplitudes of meson production in NN collisions. The reaction proceeds via excitation of $N^*(1535)$, $N^*(1650)$, and $N^*(1710)$ resonances for the η meson case and $N^*(1650)$, $N^*(1710)$ and $N^*(1720)$ for the kaon case, in the initial interactions between two nucleons. These interactions are modeled by the exchange of π, ρ, ω and σ mesons. The considered baryonic resonances have appreciable branching ratios for decays into the relevant channels. The amplitudes are calculated by summations of the Feynman diagrams generated by means of the effective Lagrangians at (a) the nucleon-nucleon-intermediate meson (NNM), (b) resonance-nucleon-intermediate meson (RNM), and (c) resonance-baryon-final meson ($RB\varphi$) vertices. The assumption entering here is that the contributions of higher-order diagrams are either negligible or they can be absorbed in the form factors of the first order diagrams.

The parameters for NNM vertices are determined by fitting the NN elastic scattering T matrix with an effective NN interaction based on π, ρ, ω and σ meson exchanges. The effective NNM Lagrangians are

$$\begin{aligned}\mathcal{L}_{NNM} = \Big[& -\frac{g_{NN\pi}}{2m_N}\bar{\Psi}_N\gamma_5\gamma_\mu\boldsymbol{\tau}\cdot(\partial^\mu\boldsymbol{\Phi}_\pi)\Psi_N \\ & - \; g_{NN\rho}\bar{\Psi}_N\left(\gamma_\mu + \frac{k_\rho}{2m_N}\sigma_{\mu\nu}\partial^\nu\right)\boldsymbol{\tau}\cdot\boldsymbol{\rho}^\mu\Psi_N \\ & - \; g_{NN\omega}\bar{\Psi}_N\left(\gamma_\mu + \frac{k_\omega}{2m_N}\sigma_{\mu\nu}\partial^\nu\right)\omega^\mu\Psi_N \\ & + \; g_{NN\sigma}\bar{\Psi}_N\sigma\Psi_N\Big], \end{aligned} \tag{1}$$

where m_N denotes the nucleon mass. Note that Eq. (1) uses a pseudovector (PV) coupling for the $NN\pi$ vertex which is consistent with the chiral symmetry requirement. Since we use these Lagrangians to directly model the T-matrix, we have also included a nucleon-nucleon-axial-vector-isovector vertex which in the limit of very large axial meson mass, cures the unphysical behavior in the angular distribution of NN scattering caused by the contact term in the one-pion exchange amplitude [36].

We introduce, at each interaction vertex, the form factor

$$F_i^{NN} = \left(\frac{\lambda_i^2 - m_i^2}{\lambda_i^2 - q_i^2}\right), i = \pi, \rho, \sigma, \omega, \tag{2}$$

where q_i and m_i are the four momentum and mass of the ith exchanged meson, respectively. The form factors suppress the contributions of high momenta and the parameter λ_i which governs the range of suppression, can be related to the hadron size. Since NN elastic scattering cross sections decrease gradually with the beam energy (beyond certain value), we take energy dependent meson-nucleon coupling constants of the following form

$$g(\sqrt{s}) = g_0 exp(-\ell\sqrt{s}), \tag{3}$$

in order to reproduce these data in the entire range of beam energies. The parameters, g_0, λ and ℓ were determined by fitting to the elastic proton-proton and proton-neutron scattering data at the beam energies in the range of 400 MeV to 4.0 GeV [36]. It may be noted that this procedure fixes also the signs of the effective Lagrangians [Eq. (1)]. The values of various parameters are given in Ref. [7]. The same parameters were used in calculations of all the inelastic channels.

We also require the effective Lagrangians for the RNM and $RB\varphi$ vertices corresponding to all the included resonances. Since the mass of the strange quark is much higher than that of the $u-$ or $d-$ quark, one does not expect the pion like strict chiral constraints for the case of other pseudoscalar mesons like η and K. Thus, one has a choice of pseudoscalar (PS) or PV couplings for the $NN\varphi$ and $R_{1/2}B\varphi$ vertices ($R_{1/2}$ corresponds to a spin-1/2 resonance). Forms of the corresponding effective Lagrangians are given in Ref. [7].

The couplings constants for the vertices involving resonances can be determined from the experimentally observed quantities such as branching ratios for their decays to corresponding channels. In most cases however, we have used the coupling constants (magnitudes as well their signs) determined in the effective Lagrangian coupled-channels analysis of the photon induced meson production reactions off nucleon reported in Refs. [33]. Since the resonances considered in this study have no known branching ratios for the decay into the $N\omega$ channel, we determine the coupling constants for the $N^*N\omega$ vertices by the strict vector meson dominance (VMD) hypothesis which is based essentially on the assumption that the coupling of photons on hadrons takes place through a vector meson. In the calculations of the amplitudes, propagators are required for intermediate mesons and nucleon resonances. These are discussed in Ref. [7].

2.2. *Final State Interaction*

For describing the data at near threshold beam energies, consideration of final state interaction (FSI) effects among the three out-going particles is important. We follow here an approximate scheme in line with the Watson-Migdal theory of

FSI [37]. In this approach the energy dependence of the cross section due to FSI is separated from that of the primary production amplitude. This is based on the assumption that the reaction takes place over a small region of space, a condition fulfilled rather well in near threshold reactions involving heavy mesons. The total amplitude is written as

$$A_{fi} = M_{fi}(NN \to NB\varphi) \cdot T_{ff}, \tag{4}$$

where $M_{fi}(NN \to NB\varphi)$ is the primary φ meson production amplitude, and T_{ff} describes the re-scattering among the final particles which goes to unity in the limit of no FSI. The factorization of the total amplitude into those of the FSI and primary production, enables one to pursue the diagrammatic approach so that the role of various meson exchanges and resonances in describing the reaction can still be investigated.

In those cases where the FSI is confined only to one particular pair of particles (mostly among baryons in case of nucleon-baryon-meson final states), T_{ff} can be calculated by following the Jost function [37] method (see, e.g., Refs. [7]). If one assumes the relative orbital angular momentum between a particular pair of particles to be zero and makes use of the effective range expansion of the corresponding phase-shift then the relevant Jost function can be related to scattering length and effective range parameters of the scattering between the two particles of that pair. In this way, comparison with data at near threshold energies provide a means to get information about low-energy scattering parameters which are otherwise not accessible for unstable particles.

In certain cases it may be necessary to include FSI among all the three outgoing particles since even if the meson-baryon interactions are weak, they can still be influential through interference. In the first reference cited under [7] expressions are derived for T_{ff} in terms of the T matrices describing FSI among all the three two-body subsystems of the final state which is obtained by following the technique of multiple FSI discussed in Ref. [38].

3. $NN \to NN\eta$ and $NN \to N\Lambda K$ and $NN \to N\Sigma K$ reactions

After having established the effective Lagrangians, coupling constants and forms of the propagators, the amplitudes for various diagrams associated with reactions under study can be calculated in straight forward manner. The isospin part is treated separately. This gives rise to a constant factor for each graph. We emphasize that signs of various amplitudes are fixed by those of the effective Lagrangian densities and coupling constants. These signs are not allowed to change anywhere in calculations.

3.1. *Check on Vertex Parameters: High Energy Data*

In any application of a model, suitability of its input parameters should be verified on a priority basis. A clean check of the vertex parameters is provided by comparison

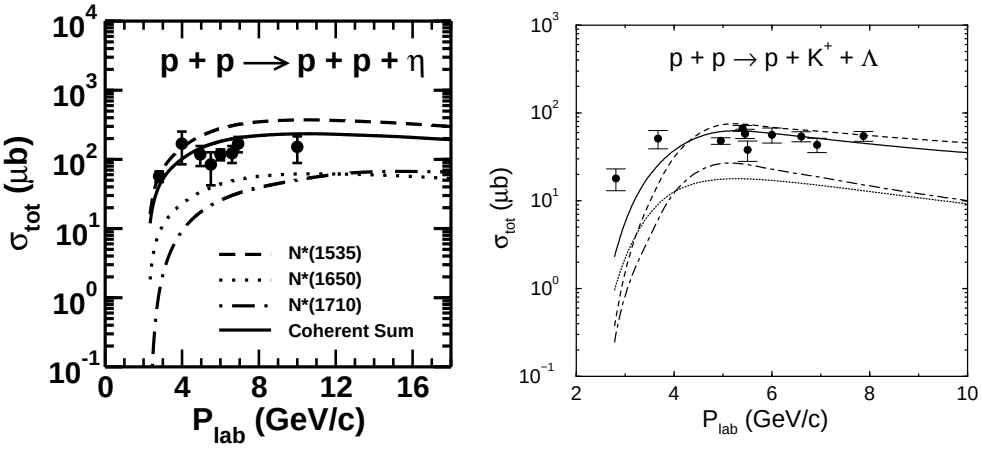

Fig. 2. Total cross sections for $p+p \to p+p+\eta$ (left) and $p+p \to p+K^+ + \Lambda$ (right) reactions as a function of beam momentum. In the left figure, dashed, dotted and dashed-dotted curves represent the contributions of $N^*(1535)$, $N^*(1650)$, $N^*(1710)$ baryonic resonance intermediate states, respectively while in the right contributions of N*(1650), N*(1710)and N*(1720) resonances are shown by dotted, dashed, and dashed-dotted lines, respectively. The coherent sum all the resonances is shown by the solid line in each case. The experimental data are from Ref. [39].

of the calculations with the data at beam momenta above 3 GeV/c as FSI effects are expected to be negligible in this region. In Fig. 2, we show comparisons of our calculations and the experimental data for total cross sections of $pp \to pp\eta$ and $pp \to p\Lambda K^+$ reactions. We see that measured cross sections are reproduced reasonably well by our calculations (solid line) in the entire range of beam momenta. This fixes the parameters of all the vertices. In the application of our model to describe these reactions at near threshold beam energies, the amplitude $M_{fi}(NN \to NB\varphi)$, has been calculated with exactly the same values for all the vertex parameters.

We further notice that while contributions of the $N^*(1535)$ resonance dominates $pp \to pp\eta$ reaction for all the beam momenta, the $pp \to p\Lambda K^+$ reaction is dominated by the $N^*(1710)$ and $N^*(1650)$ excitations above and below 3 GeV/c beam momentum, respectively. However, in both cases, the interference terms of the amplitudes corresponding to various resonances are not negligible.

3.2. *Strangeness production at near threshold beam energies: Role of Final State Interactions*

Several groups have measured the cross sections for $pp \to pp\eta$, $pp \to p\Lambda K^+$, $pp \to p\Sigma^0 K^+$, $pp \to n\Sigma^+ K^+$ and $pp \to p\Sigma^+ K^0$ reactions at beam energies very close to their respective production thresholds (see, e.g, Ref. [8] for references upto 2002 and Refs [10,11] for more recent studies). The data are usually presented as functions of kinetic energy in the exit channel. We define the excess energy of the reaction as $\varepsilon = \sqrt{s} - m_p - m_B - m_\varphi$, where $\sqrt{s}$ is the invariant mass. At near thresh-

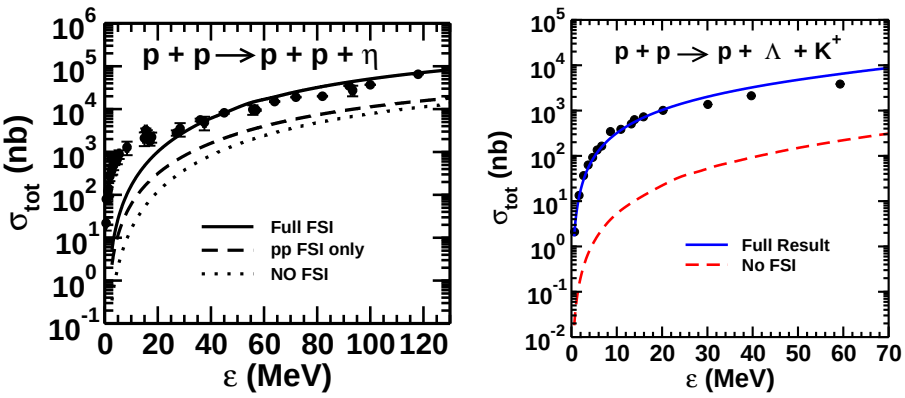

Fig. 3. The total cross section for $pp \to pp\eta$ (left) and $pp \to p\Lambda K^+$ (right) reactions as a function of the excess energy. In the left panel dotted and dashed curves represent cross section obtained with FSI effects included only in the proton-proton sub-state of the final channel and no FSI at all, respectively. In the right panel results obtained with no FSI effects are shown by dashed lines. The solid line shows the results obtained with full FSI effects.

old beam energies, the outgoing particles have small relative momenta. Therefore, interpretation of the data requires a correct treatment of the final state interactions among the final channel particles.

In Fig. 3, we present comparisons of our calculations with the experimental data for total cross sections of $pp \to pp\eta$ and $pp \to p\Lambda K^+$ reactions as a function of ε. For both reactions the FSI effects are important at these low beam energies. While, for the $pp \to p\Lambda K^+$ reaction our model is able to describe the data well for the entire range of beam energies, for the $pp \to pp\eta$ reaction data are reproduced only for ε values in the range of 15 - 130 MeV. However, for the later case, an important result is that the FSI in the ηp sub-state is indeed quite important in our model. Yet it is not enough to explain the data for $\varepsilon < 15$ MeV. Underpredition of the data by theory for these values of ϵ, has also been seen in calculations presented in Refs. [40].

There may be several reasons for this underprediction. ηp final state interaction may have a different form for these low energy which could make it relatively stronger in this region. We noted that taking larger values for the scattering lengths $a_{\eta N}$ worsens the fit to the data for $\varepsilon > 15$ MeV. In fact, best description of the data is provided by the ηN scattering amplitudes corresponding to $a_{\eta N} = 0.51 + i0.26$. Although, the real part of this $a_{\eta N}$ is about half of that of the "preferred" $\eta - N$ parameter set of Ref. [41], yet a smaller $a_{\eta N}$ is consistent with that extracted by several authors [31,42,43,44,30] from studies involving meson-nucleon scattering. On the other hand, calculations of FSI effects within the three-body scattering theory of Faddeev type [45] seem to reproduce the data for $\varepsilon < 15$ Mev. However, predictions of this theory for $\varepsilon > 60$ MeV is not known.

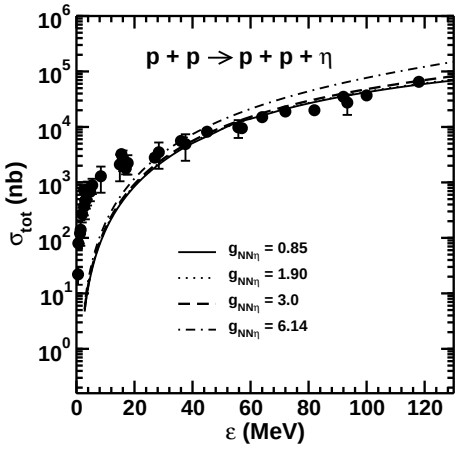

Fig. 4. The total cross section for the $pp \to pp\eta$ reaction including the Born term (nucleon intermediate states) as function of ε. Results are shown for different values of $g_{NN\eta}$.

The Born term (nucleon intermediate states) is conjectured to contribute strongly at lower energies. To check this point we present in Fig. 4 results of our full calculations with Born term included. We see that the inclusion of the amplitudes corresponding to the nucleon intermediate states, makes negligible difference to the results shown in Fig. 3 if the value of the coupling constant $g_{NN\eta}$ is below 3.0. Using the largest considered value of for $g_{NN\eta}$ (6.14), the results are affected to the extent of only a few percent. Obviously, due to considerable amount of uncertainty in the value of $g_{NN\eta}$, the nucleon excitation amplitudes are quite uncertain and their inclusion makes no significant difference in the results reported in Fig. 3. In particular, the discrepancy between theory and the data for $\epsilon < 15$ MeV remains unresolved.

Recently, it has been shown [46] that the description of the $pp \to pp\eta$ data can be improved considerably for lower values of ε within a resonance model by including $D_{13}(1520)$ resonance with unusually large couplings constants for for $RN\rho$ and $RN\omega$ vertices. In this context one should note that coupling constants extracted in the effective Lagrangian coupled-channels analysis [35,47] of $\pi N \to \omega N$ and $\gamma N \to \rho N$ reactions are about an order of magnitude smaller than those used in Ref. [46]. We believe that explanation of the $pp\eta$ data for beam energies very close to the threshold is still an open issue.

The production of light hyperons in proton-proton collisions has been extensively studied at close-to-threshold beam energies. The energy dependence of the experimental total cross sections of $pp \to p\Lambda K^+$ and $pp \to p\Sigma^0 K^+$ reactions has been well reproduced within the effective Lagrangian model (see, last of Ref. [7]). Very recently, data have become available also for the $pp \to n\Sigma^+ K^+$ reaction. The interest in the Σ^+ production channel stems from the fact that it provides a sen-

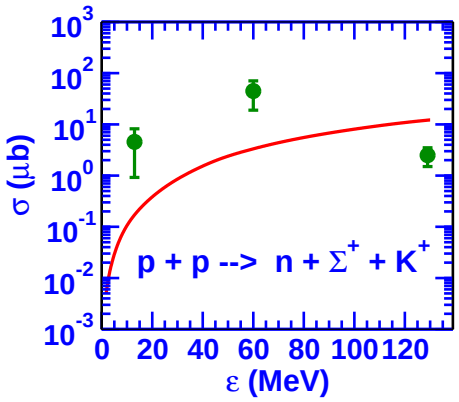

Fig. 5. The total cross section for the $pp \to n\Sigma^+K^+$ reaction as a function of excess energy (ε). The experimental data for ε values of 13 MeV and 60 MeV are taken from [10] and that at 129 MeV is from [11].

sitive tool to search for a possible penta quark state. COSY-11 and COSY-ANKE collaborations have reported quite contrasting values for this reaction at excess energies of 13 MeV and 60 MeV [10], and 129 MeV [11], respectively.

In Fig. 5, we compare these data with predictions of our model. We notice that lower energy data points are surprisingly too high - they are at least an order of magnitude larger than our calculations. On the other hand, the higher energy point is smaller than the theoretical results by a factor of about 3. Two measurements, thus, imply a very large threshold anomaly which must be verified. It has been suggested that inclusion in production process of the $\Delta(1620)$ resonance and an unrealistically very strong $n\Sigma^+$ FSI would allow to achieve a much better agreement (within factors of 2-4) with the data at lower energies [48]. However, in this calculation, the coupling constant for the $\Delta N\Sigma$ vertex is very uncertain. While there is no creditable evidence for the decay of $\Delta(1620)$ isobar into the $n\Sigma^+$ channel, there are branching ratios known (albeit with large error bars) for the decay of $\Delta(1600)$ and $\Delta(1920)$ isobars into this channel [49]. One should rather include these resonances into the model. In any case, the calculations of Ref. [48] grossly overpredicts the data point at high energy. The solution of this problem must await the new measurements of this reaction by the COSY-ANKE group at close-to-threshold energies.

4. Summary and Conclusions

In summary, we presented some application of our effective Lagrangian model in understanding the recent data on hidden strangeness production ($NN \to NN\eta$) and open strangeness production ($pp \to p\Lambda K^+$, $pp \to p\Sigma^0K^+$, $pp \to n\Sigma^+K^+$) reactions in nucleon-nucleon collisions. With the same set of vertex parameters, the model is able to provide a good description of the $pp \to pp\eta$ reaction at higher as

well as near threshold beam energies except for the excess energies below 15 MeV where our calculations underpredict the experimental cross sections. We examined the validity of several suggestions for understanding this discrepancy. It turns out that a very strong ηN FSI or the inclusion of the Born term is unlikely to explain this anomaly. Inclusion of the $D_{13}(1520)$ resonance with reasonable coupling constants at the vector meson vertices is also unlikely to be of any help. This at the moment remains an open issue.

This model is able to describe majority of the data on $pp \to p\Lambda K^+$ and $pp \to p\Sigma^0 K^+$ reactions where it is found that the $N^*(1650)$ resonant state contributes predominantly to both these reactions at near threshold beam energies. Therefore, the study of these reactions provides an ideal means of investigating the properties of this S_{11} baryonic resonance. On the other hand, calculations are not compatible with the published few data points on $pp \to n\Sigma^+ K^+$ reaction. One has to wait for the results of the new measurements for this reaction by the COSY-ANKE group at near threshold beam energies.

5. Acknowledgments

The author wishes the thank Hans Ströher for several useful conversations on the measurements of the COSY-ANKE group.

References

1. K. G. Wilson, Phys. Rev. **D10**, 2445 (1974).
2. T. Burch, C. Gattringer, L. Ya. Glozman, C. Hagen, D. Hierl, C. B. Lang, and A. Schäfer, Phys. Rev. D. **74**, 014504 (2006).
3. D. B. Leinweber, W. Melnitchouk, D. G. Richards, A. G. Williams, and L. M. Zanotti, in *Lattice Hadron Physics*, edited by A. Kalloniatis, D. Leinweber, A. Williams (Springer, Berlin, 2005), P. 71; J. M. Zanotti, B. Lasscock, D. B. Leinweber and A. G. Williams, Phys. Rev. **D71**, 034510 (2005); R.D. Young, D. B. Leinweber, and A. W. Thomas, Phys. Rev. **D71**, 014001 (2005).
4. S. Capstick and W. Roberts, Prog. Part. Nucl. Phys. **45**, 241 (2000).
5. U. Löring, K. Kretzschmar, B. C. Metsch, H. R. Petry, Eur. Phys. J A **10**, 395 (201).
6. M. F. M. Lutz and E. E. Kolomeitsev, Nucl. Phys. **A755**, 29 (2005); J. Hofmann and M. F. M. Lutz, Nucl. Phys. **A763**, 90 (2005); J. Hofmann and M. F. M. Lutz, Nucl. Phys. **A776**, 17 (2006).
7. R. Shyam, Phys. Rev. C **75**, 055201 (2007); R. Shyam, *ibid* **60**, 055213 (1999); R. Shyam, G. Penner and U. Mosel, *ibid* **63**, 022202(R) (2001); R. Shyam, *ibid.***73**, 035211 (2006).
8. P. Moskal, M. Wolke, A. Khoukaz, and W. Oelert, Progr. Part. Nucl. Phys. **49**, 1 (2002) and references therein of previous studies.
9. A. Abd El-Samad *et al.*, Phys. Lett. **B632**, 27 (2006) and refrences therein
10. T. Rozek *et al.*, Phys. Lett. **B643**, 251 (2006) and references therein.
11. Yu. Valdau *et al.*, Phys. Lett. **B652**, 245 (2007) and references therein.
12. T.E.O Ericson and W. Weise, *Pions and Nuclei*, Clarendon, Oxford, 1988; V. Bernard, N. Kaiser, and Ulf-G. Meissner, Int. J. Mod. Phys. **E4**, 193 (1995); C. Hahnhart, Phys. Rep. **397**, 155 (2004).

13. M. Alberg, Prog. Part. Nucl. Phys. **36**, 217 (1996.
14. C. Dover and P. Fishbane, Phys. Rev. Lett. **64**, 3115 (1990).
15. A. Deloff, Nucl. Phys. **A505**, 583 (1989).
16. N. Mathur, Y. Chen, S. J. Dong, T. Draper, I. Horvath, F. X. Lee, K. F. Liu, and J. B. Zhang, Phys. Lett. B **605**, 137 (2005)
17. U. Mosel, Annu. Rev. Nucl. Part. Sci. **41**, 29 (1991) and references therein.
18. J. Aichelin, Phys. Rep. **202**, 233 (1991).
19. W. Cassing and E. Bratkovskaya, Phys. Rep. 308, 65 (1999).
20. E.L. Bratkovskaya, M. Bleicher, W. Cassing, M. van Leeuwen, M. Reiter, S. Soff, H. Stöcker, and H. Weber, Prog. Part. Nucl. Phys. **53**, 225 (2004).
21. P. Danielewicz, R. Lacey and W.G. Lynch, Science, **209**, 1592 (2002).
22. C.M. Ko, V. Koch, G.Q. Li, Annu. Rev. Nucl. Part. Sci, **47**, 505 (1997.
23. P. Senger, Acta, Phys. Pol, B **39**, 321 (2008.
24. J. Rafelski and B. Müller, Phys. Rev. Lett. **48**, 1066 (1982); J. Rafelski, arXiv:0710.1931 [EPJ-ST **155**, 139 (2008)].
25. H.C. Chiang, E. Oset, and L.C. Liu, Phys. Rev. C **44**, 738 (1991).
26. A. Fix and H. Arenhövel, Phys. Rev. C **66**, 024002 (2002).
27. Q. Haider and L.C. Liu, Phys. Rev. C **66**, 045208 (2002).
28. M. Pfeiffer et. al., Phys. Rev. Lett. **92**, 252001 (2004).
29. A. Sibirtsev, J. Haidenbauer, J.A. Niskanen, and U.-G. Meissner, Phys. Rev. C **70**, 047001 (2004).
30. J. Durand, B. Juli-Daz, T.-S. H. Lee, B. Saghai, T. Sato, arXiv:0804.3476.
31. T. Feuster and U. Mosel, Phys. Rev.C **58**, 457 (1998);*ibid,* Phys. Rev.C **59**,460 (1999).
32. A. Yu. Korchin, O. Scholten, and R. G. E. Timmermans, Phys. Lett. **B438**, 1 (1998).
33. G. Penner and U. Mosel, Phys. Rev. C **66**, 055211 (2002); **66**, 055212 (2002);
34. A. Usov and O. Scholten, Phys. Rev. C**72**, 025205 (2005).
35. V. Shklyar, H. Lenske, U. Mosel, and G. Penner, Phys. Rev. C **71**, 055206 (2005).
36. M. Schäfer, H.C. Dönges, A. Engel and U. Mosel, Nucl. Phys. **A575**, 429 (1994).
37. M.L. Goldberger and K.M. Watson, *Collision Theory*, Wiley, New York, 1969, pp 549.
38. J. Gillespie, *Final-State Interaction*, Ed. K. M. Watson, Holden-Day Adv. Phys. Monographs, Holden-Day, San Francisco, 1964, and references therein.
39. *Landolt-Börnstein: Numerical Data and Functional Relationships in Science and Technology, New Series*, edited by H. Schopper, I/12 (Springer, Berlin, 1988).
40. K. Nakayama, J. Speth, and T.-S. H. Lee, Phys. Rev. C, **65**, 045210 (2002); K. Nakayama, J. Haidenbauer, C. Hanhart, and J. Speth, Phys. Rev. C **68**, 045201 (2003).
41. A. M. Green, and S. Wycech, Phys. Rev. C **71**, 014001 (2005).
42. H. Galcilazo amd M. T. Pena, Phys. Rev. C **66**, 034606 (2002).
43. M.F.M. Lutz, G. Wolf, and B. Friman, Nucl. Phys. **A706**, 431 (2002).
44. A. M. Gasparyan, J. Haidenbauer, C. Hanhart, and J. Speth, Phys. Rev. C **68**, 045207 (2003).
45. A. Fix and H. Arenhövel, Phys. Rev. C **69**, 014001 (2004).
46. K. Nakayama, Y. Oh, and H. Haberzettl, arXiv:0803.3169 [hep-ph].
47. A. Usov and O. Scholten, Phys. Rev. C **74**, 015205 (2996).
48. J.J. Xie and B.S. Zou, Phys. Lett. **B649**, 405 (2007).
49. W.M. Yao et. al. (particle data group), J. Phys. G: Nucl & Part. Phys. **33**, 1 (2006).